A simplified and highly efficient cell-free protein synthesis system for prokaryotes

Xianshengjie Lang[1,#], Changbin Zhang[1,#], Jingxuan Lin[1], Zhe Zhang[1,*], Wenfei Li[1,2,*]

[1] School of Basic Medical Sciences, Cheeloo College of Medicine, Shandong University, Jinan, Shandong, China.

[2] Children's Hospital Affiliated to Shandong University, Jinan, Shandong, China.

[#] Equal contribution

[*] Correspondence to: Zhe Zhang zhezhang@sdu.edu.cn, Wenfei Li wenfeili@sdu.edu.cn

Abstract

Cell-free protein synthesis (CFPS) systems are a powerful platform with immense potential in fundamental research, biotechnology, and synthetic biology. Conventional prokaryotic CFPS systems, particularly those derived from *Escherichia coli* (*E. coli*), often rely on complex reaction buffers containing up to thirty-five components, limiting their widespread adoption and systematic optimization. Here, we present an optimized *E. coli* cell-free protein synthesis (*e*CFPS) system, which is significantly streamlined for high efficiency. Through systematic screening, we successfully reduced the essential core reaction components from 35 to a core set of 7. The thorough optimization of these seven key components ensured that protein expression levels were not only maintained but even substantially improved. Furthermore, we developed a much simpler procedure for preparing the bacterial cytosolic extracts, a "fast lysate" protocol that eliminates the traditional time-consuming runoff and dialysis steps, thereby enhancing the overall accessibility and robustness of *e*CFPS. This optimized and user-friendly *e*CFPS efficiently synthesizes challenging proteins, including functional, self-assembling vimentin, and active restriction endonuclease *Bsa*I despite its strong cytotoxicity, and serves as a powerful tool that will facilitate diverse applications in basic life science research and beyond.

Introduction

Cell-free protein synthesis (CFPS) offers a powerful and flexible platform for biological research and biotechnological applications by reproducing the cellular protein synthesis process in an *in vitro* environment[1,2]. Compared to traditional cell-based expression systems, CFPS possesses several notable advantages, including rapid reaction kinetics, ease of operation, independence from cell culture, high tolerance to toxic proteins, and facile incorporation of non-canonical amino acids[3–5]. These characteristics position CFPS for broad applications in protein engineering, high-throughput screening, synthetic biology, and diagnostic reagent development[6,7].

Prokaryotic CFPS systems, especially those based on *E. coli* lysates, have garnered significant attention for their high protein synthesis yields and compatibility with genetic manipulations[8–13]. They have played a pivotal role in early molecular biology research and continue to be relevant in industrial protein production and biosensor development[1,14–16]. However, for a long time, most prokaryotic CFPS protocols have relied on complex buffer systems containing a large number of auxiliary components[17,18]. A comprehensive analysis of existing literature reveals that the composition of reaction buffers differs widely between protocols, both in the number of optional components and in the concentrations of individual components (**Table S1**). These complex systems, while effective, often lead to high costs, laborious preparation procedures, and potential interactions among components, posing significant challenges for further optimization and standardization, thereby limiting their widespread adoption in resource-constrained laboratories.

In recent years, the field of eukaryotic CFPS has seen remarkable progress in system optimization and simplification[19,20]. Highly optimized human *in vitro* translation systems have demonstrated that high-efficiency protein synthesis can be achieved with a minimal number of core components[19]. Recognizing the potential of such systematic optimization approaches, we hypothesized that similar strategies could be equally applicable and beneficial for *E. coli* CFPS systems by thoroughly analyzing the functions of existing components and integrating insights from previous reports on prokaryotic protein synthesis mechanisms. This study aimed to develop a highly simplified yet efficient *E. coli*

60 cell-free protein synthesis system (*e*CFPS). We conducted a systematic component
61 reduction screening of traditional *e*CFPS systems, successfully streamlining the core
62 components from thirty-five to just seven. The subsequent meticulous optimization of
63 these seven key components not only maintained but even improved protein expression
64 levels. Through these dual efforts—simplifying the reaction mixture and developing a
65 high-quality, dialysis-free "fast lysate" preparation—we established a highly accessible
66 and robust *e*CFPS platform which will accelerate diverse applications in life science
67 research.

68

69 **Results**

70 **Streamlining *e*CFPS: removal of dispensable components**

71 To develop a more streamlined and efficient *e*CFPS system, we performed a systematic
72 screening of auxiliary components commonly found in traditional prokaryotic CFPS
73 protocols[17,21]. Our objective was to identify dispensable components while maintaining or
74 enhancing protein synthesis efficiency, thereby simplifying system preparation and
75 reducing costs. Starting with a comprehensive reaction mixture containing up to thirty-five
76 components[17], we iteratively evaluated the contribution of individual constituents through
77 luciferase reporter assays. Throughout this optimization, essential core components such
78 as creatine phosphate (CrP), creatine kinase (CrK), ATP, GTP, magnesium, and
79 potassium were maintained in the base reaction mixture[3,8,19]. Our systematic approach
80 allowed us to precisely determine the impact of each component on overall protein
81 synthesis yield, leading to the identification of both dispensable and critical factors.

82 Through this systematic screening, we first identified several components that could be
83 entirely removed from the reaction mixture without compromising protein synthesis
84 efficiency (**Figure 1**). Dithiothreitol (DTT), a reducing agent commonly included in both
85 transcription and translation systems to maintain protein sulfhydryl groups in a reduced
86 state and prevent aggregation, was found to be unnecessary within our specific system,
87 as its removal did not affect the final protein expression levels (**Figure 1A**). Similarly,
88 cyclic adenosine 3′,5′-monophosphate (cAMP), a regulator implicated in transcriptional
89 regulation[22–24], was also found to be dispensable for efficient protein synthesis (**Figure**

90 **1B**). Furthermore, we systematically evaluated other auxiliary components, including the
91 molecular crowder polyethylene glycol 8000 (PEG8000), used to enhance
92 macromolecular crowding[25–29]; ammonium ions (NH_4^+), typically included as an osmolyte
93 and for its role in maintaining protein stability and solubility in *e*CFPS reactions[29–33]; and
94 folinic acid, which serves as a crucial cofactor for nucleotide synthesis[8,33]. Our results
95 consistently showed that removing these components had a negligible impact on overall
96 protein synthesis performance (**Figure 1C-E**). These findings collectively demonstrate
97 that a substantial portion of the auxiliary components in traditional *e*CFPS protocols can
98 be eliminated, paving the way for a more streamlined and cost-effective system.

99 An evaluation of various concentrations of amino acids and tRNA was conducted, as
100 these components are fundamental building blocks for protein synthesis[34–36]. Previous
101 studies on *e*CFPS have highlighted the rapid degradation of certain amino acids, such as
102 arginine, cysteine, and tryptophan, necessitating their replenishment for prolonged
103 synthesis[37,38]. Our results showed that while these components are critical for achieving
104 high yields, protein synthesis still occurs in their absence (**Figure 1F-G**). This suggests
105 that while they are optimizable, tRNA and amino acids are not strictly essential for the
106 reaction to proceed, likely due to residual amounts within the cell lysate (**Figure 1F-G**).
107 Furthermore, we evaluated the role of nucleoside triphosphates (NTPs) in our system,
108 which are essential for coupled transcription-translation. Interestingly, we found that
109 protein synthesis could proceed without the addition of CTP or UTP (**Figure 1H-I and**
110 **Figure S1**). While adding either ATP or GTP alone resulted in a very weak reaction, the
111 presence of both ATP and GTP together recovered the reaction to approximately 40% of
112 the complete NTPs mix (**Figure S1B-C**). This highlights the critical role for ATPase-
113 dependent chaperones (e.g., DnaK) and GTPase-dependent elongation factors (e.g., EF-
114 Tu and EF-G)[39], which are crucial for proper protein folding during synthesis[40].

115 Ultimately, this comprehensive screening allowed us to successfully reduce the core
116 reaction components from thirty-five to just seven (**Figure 1J**).
117 .
118

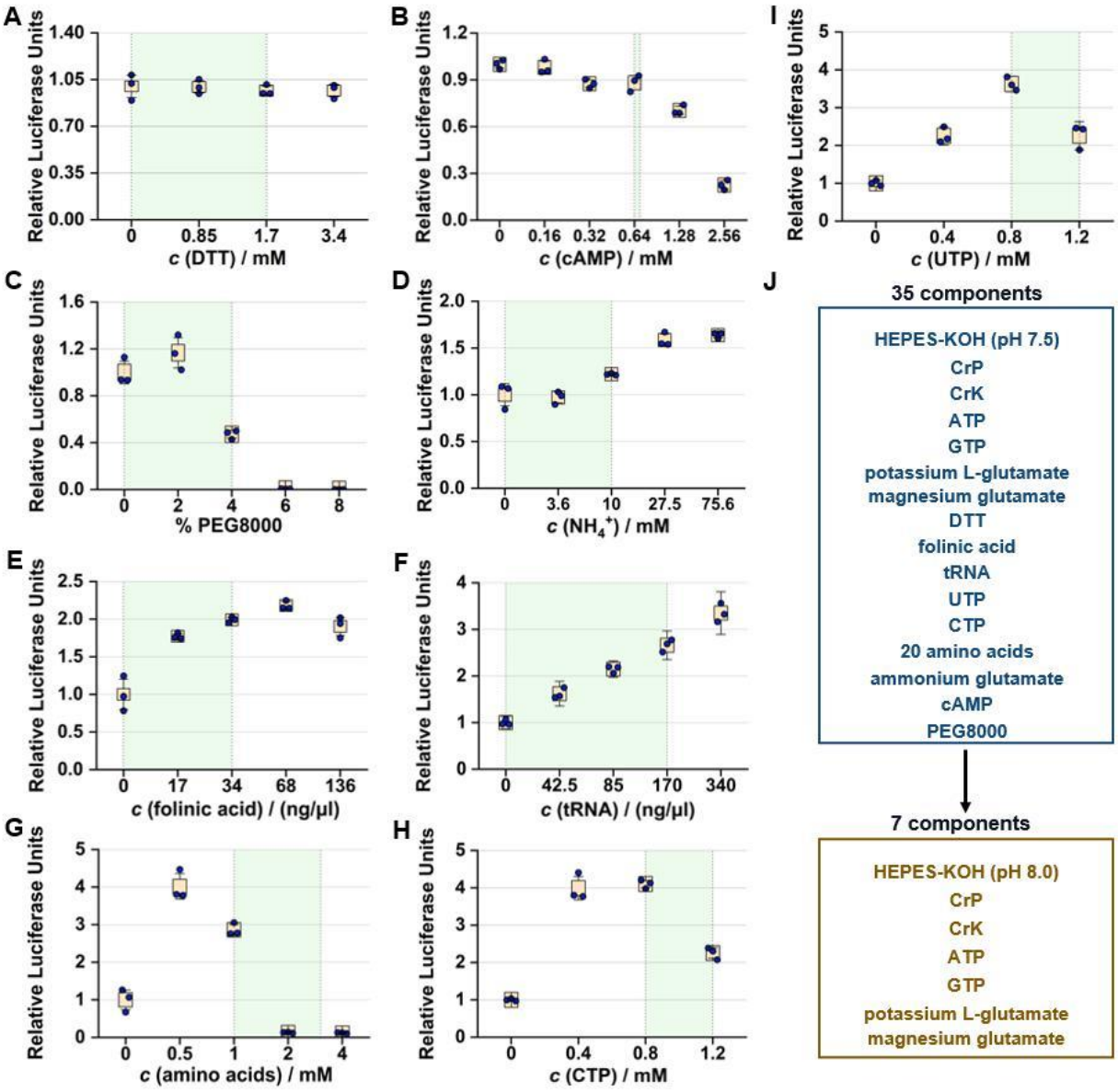

Figure 1 Optimization of *e*CFPS components. Protein expression levels from the *e*CFPS system were measured using an Nanoluciferase (NLuc) reporter DNA. Green area in the graphs indicate the common concentration range used in published protocols for *e*CFPS. Error bars represent the standard error (SE) of at least three independent reactions. (**A-E**) Protein expression levels of the *e*CFPS system supplemented with different concentration of DTT (**A**), cAMP (**B**), PEG8000 (**C**), NH_4^+ (**D**), and folinic acid (**E**). (**F-I**) Protein expression levels of *e*CFPS with various concentrations of tRNA (**F**), amino acids (**G**), CTP (**H**) and UTP (**I**). (**J**) A summary of the supplement components before and after optimization.

Optimization of essential *e*CFPS components

129 While a core set of seven components was found to be sufficient for protein synthesis,
130 we conducted further fine-tuning to maximize the system's performance. First, we
131 optimized the concentrations of key salts and energy components (**Figure 2**). Our findings
132 reveal that the final protein expression level is highly dependent on the concentrations of
133 both magnesium (Mg^{2+}) and potassium ions (K^{+}), which are fundamental for the structural
134 integrity and catalytic activity of ribosomes, and various enzymatic reactions critical to
135 *e*CFPS[41,42]. Through a detailed matrix-based optimization, we first identified the optimal
136 concentrations of Mg^{2+} and K^{+} to achieve maximum protein expression (**Figure 2A**).
137 Similarly, we conducted a separate screen to optimize the concentrations of Mg^{2+} and
138 PEG8000 as previous reports have suggested a cooperative relationship between them[17]
139 (**Figure 2B**).

140 A comprehensive evaluation of the core energy components was also performed. We
141 specifically focused on co-optimizing the concentrations of ATP and GTP, which serve as
142 both energy sources and building blocks[43–45], to maximize the yield of protein synthesis
143 (**Figure 2C**). Additionally, the energy regeneration system, primarily composed of CrP
144 and CrK, is vital for maintaining sustained ATP levels[46,47]. We found that CrP is crucial,
145 with no reaction occurring in its absence (**Figure S2A**). Initial experiments showed that
146 while CrK addition significantly boosted translation efficiency early on, reactions without
147 exogenous CrK could achieve a protein expression level approximately four times higher
148 at later time points (2 hours or more), suggesting the presence of an endogenous CrK-
149 like enzyme in the lysate (**Figure S2B**). A co-optimization screen for CrP and CrK
150 concentrations was also performed, and our results showed that optimizing the
151 concentrations of these components is critical for achieving and sustaining high protein
152 expression (**Figure 2D**). Furthermore, we optimized the pH and concentration of the
153 HEPES buffer, finding that a specific range was critical for maintaining stable and high
154 protein expression (**Figure 2E**). These multi-faceted optimizations ensured that each
155 component was present at its ideal concentration, leading to a synergistic effect that
156 significantly boosted the system's overall performance.

157

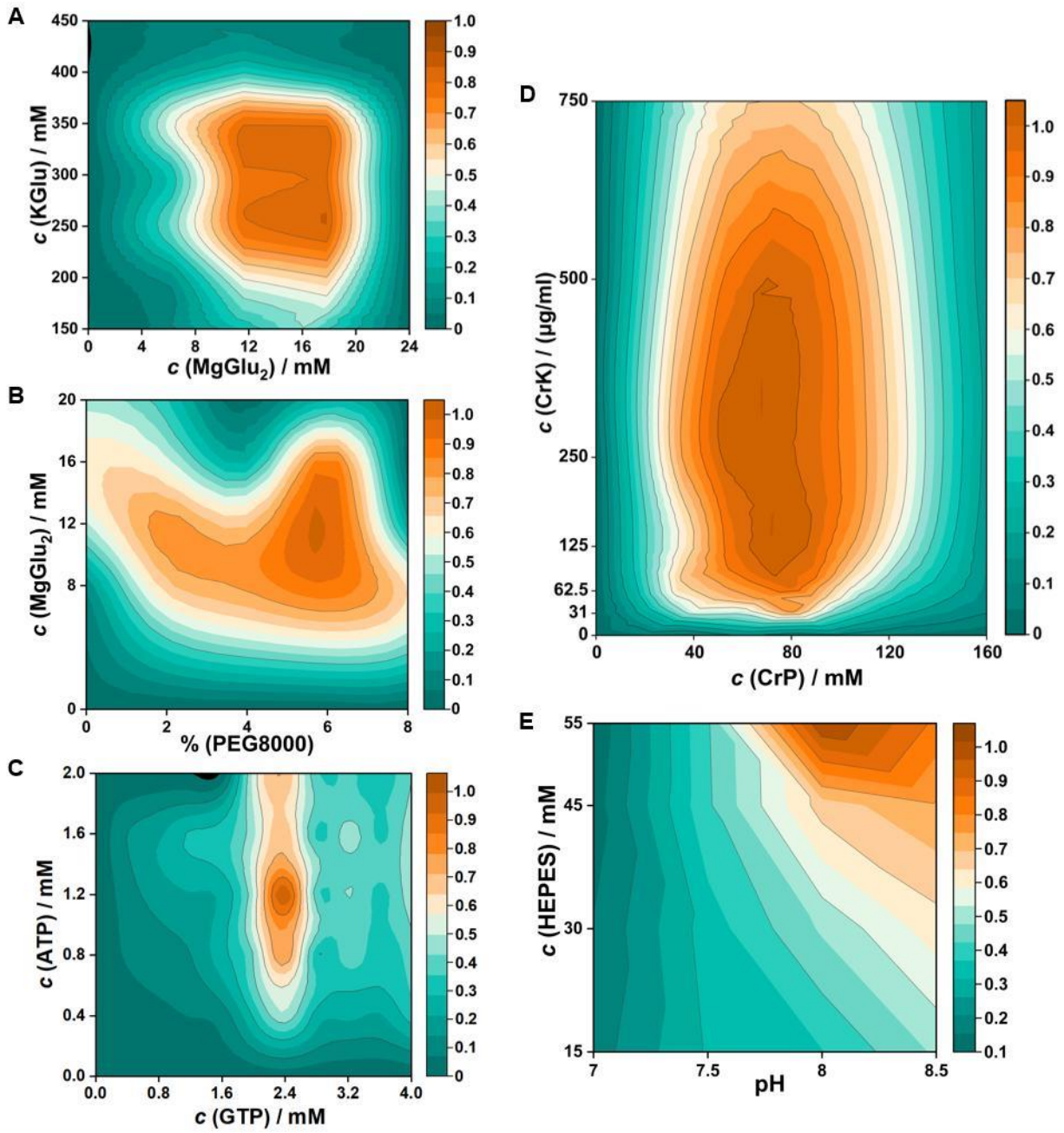

158

159 **Figure 2 Optimization of essential components for *e*CFPS system.** (**A**) Protein
160 expression levels of the *e*CFPS system measured at varying concentrations of KGlu and
161 $MgGlu_2$. (**B**) Protein expression levels of the *e*CFPS system measured at varying
162 concentrations of $MgGlu_2$ and PEG8000. (**C**) Protein expression levels of the *e*CFPS
163 system measured at varying concentrations of ATP and GTP. (**D**) Protein expression
164 levels of the *e*CFPS system measured at varying concentrations of CrK and CrP. (**E**)

165 Protein expression levels of the *e*CFPS system measured at varying pH and buffer
166 concentrations. Data from all panels present mean ± SE, n = 3.

167 **Performance characterization of the optimized *e*CFPS**

168 To thoroughly evaluate the performance of our optimized *e*CFPS, we conducted a series
169 of experiments. We first investigated the kinetics of protein synthesis measuring the
170 expression over time at different temperatures (25°C, 30°C, and 37°C). Our results
171 demonstrate that the system exhibits robust protein synthesis across this range, with the
172 highest expression rates observed at the physiological temperature of 37°C (**Figure 3A**).
173 Next, we assessed the system's sensitivity to DNA concentration, finding that it could
174 efficiently utilize a wide range of reporter DNA templates to produce quantifiable protein
175 products, which were validated by both luminescence assays and western blot analysis
176 (**Figure 3B**). Furthermore, we investigated the impact of varying cell lysate volume ratios,
177 comparing our initial system with the newly optimized *e*CFPS. Our findings indicate that
178 the optimized system maintains superior protein expression even at different lysate-to-
179 buffer ratios (**Figure 3C**).

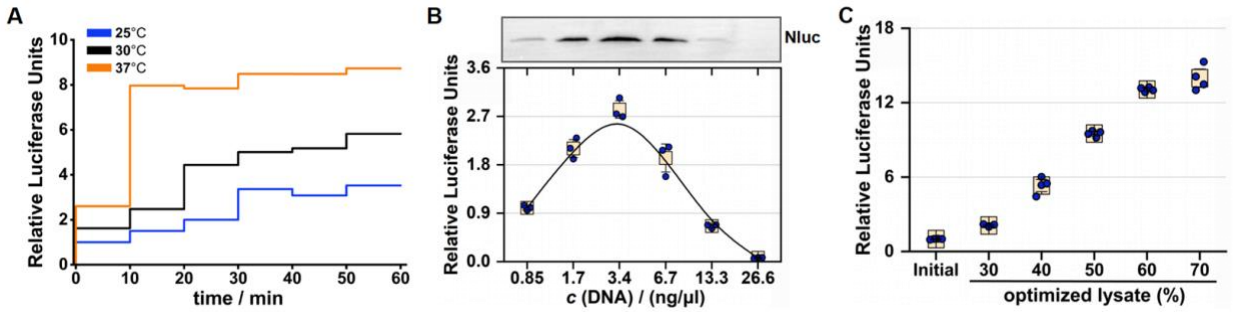

180

181 **Figure 3 Characterization of the optimized *e*CFPS system.** (**A**) Kinetics of protein
182 synthesis at 25°C, 30°C and 37°C over a 60-minute period. Data present mean ± SE, n
183 = 3. (**B**) Protein expression levels of the *e*CFPS system measured at varying DNA
184 concentrations for a reporter encoding a FLAG-tagged NLuc. The protein product was
185 quantified via a luminescence assay and confirmed by western blotting. Data present
186 mean ± SE, n = 3. (**C**) Comparison of protein expression levels from the initial and
187 optimized *e*CFPS systems at various cell extract volume ratios. Data present mean ± SE,
188 n = 4.

189 **Comparative analysis of energy regeneration systems and expression of**
190 **challenging proteins**

191 To validate the efficacy of our optimized *e*CFPS, we benchmarked its performance
192 against two widely used systems: the classical Phosphoenolpyruvate (PEP)-based
193 energy system, a common alternative for ATP regeneration [6,7], and an initial CrP/CrK-
194 based system (**Figure 4**). We utilized NLuc, representing a broadly applicable protein,
195 and super-folder green fluorescent protein (sfGFP), with codons optimized for *E. coli* as
196 reporter proteins and monitored their expression over time (**Figure 4A-B, Figure S3A**).
197 Our results show that the optimized *e*CFPS consistently outperforms both the classical
198 and initial systems, achieving significantly higher protein expression levels in a shorter
199 period (**Figure 4A-B**). The robust expression was further confirmed by western blot
200 analysis, which provided clear visual evidence of the superior protein yield from our
201 optimized system (**Figure 4C-D, Figure S3B-C**). Finally, we validated the function of our
202 system through antibiotic-mediated inhibition assays. Our results demonstrate that
203 protein expression in the optimized *e*CFPS can be effectively inhibited by standard
204 antibiotics, confirming its robust and native-like translation machinery (**Figure S3D**).

205 To further validate the system's capability in synthesizing challenging, functional proteins,
206 we focused on the restriction endonuclease *Bsa*I (**Figure 4E-F**). Restriction
207 endonucleases like *Bsa*I are notoriously difficult to express *in vivo* due to their specific
208 DNA-cleaving activity, which is highly cytotoxic to the host *E. coli* cells. Traditional
209 recombinant expression requires the compulsory co-expression of a corresponding
210 methylase to protect the host genome, adding significant complexity to the system[48,49].
211 Leveraging the inherent cell-free advantage of circumventing cytotoxicity, we first
212 demonstrated the system's utility by synthesizing the restriction endonuclease *Bsa*I[50],
213 confirming its specific enzymatic activity via a DNA cleavage assay, which underscores
214 the system's ability to produce complex, functional enzymes (**Figure 4E-F**). We confirmed
215 that the *e*CFPS synthesized *Bsa*I was functionally active, successfully cleaving its
216 substrate plasmid DNA (**Figure 4F**). Based on the standard definition of enzyme activity
217 (1 U digests 1 μg of substrate DNA in 20 μL at 37°C in 1 h), we calculated the enzyme
218 activity of our *e*CFPS-produced *Bsa*I to be in the range of $2\times10^3 \sim 2\times10^4$ U/mg (**Figure**

219 4F). The efficient production of this active enzyme demonstrates the power of our
220 simplified system for producing complex, cytotoxic proteins.

221 Next, we successfully expressed vimentin, an intermediate filament protein (Figure 4G).
222 Vimentin is a type III intermediate filament protein that forms part of the cytoskeleton[51]. It
223 is known to be difficult to express and handle due to its high propensity for aggregation.
224 Our *e*CFPS system efficiently expressed vimentin **(Figure 4G).** Crucially, the vimentin
225 expressed in our CFPS system demonstrated successful *in vitro* self-assembly into
226 filaments (Figure 4H), which was confirmed by negative-stain electron microscopy,
227 confirming the system's robust performance even for difficult-to-express, aggregation-
228 prone proteins (Figure 4E-H).

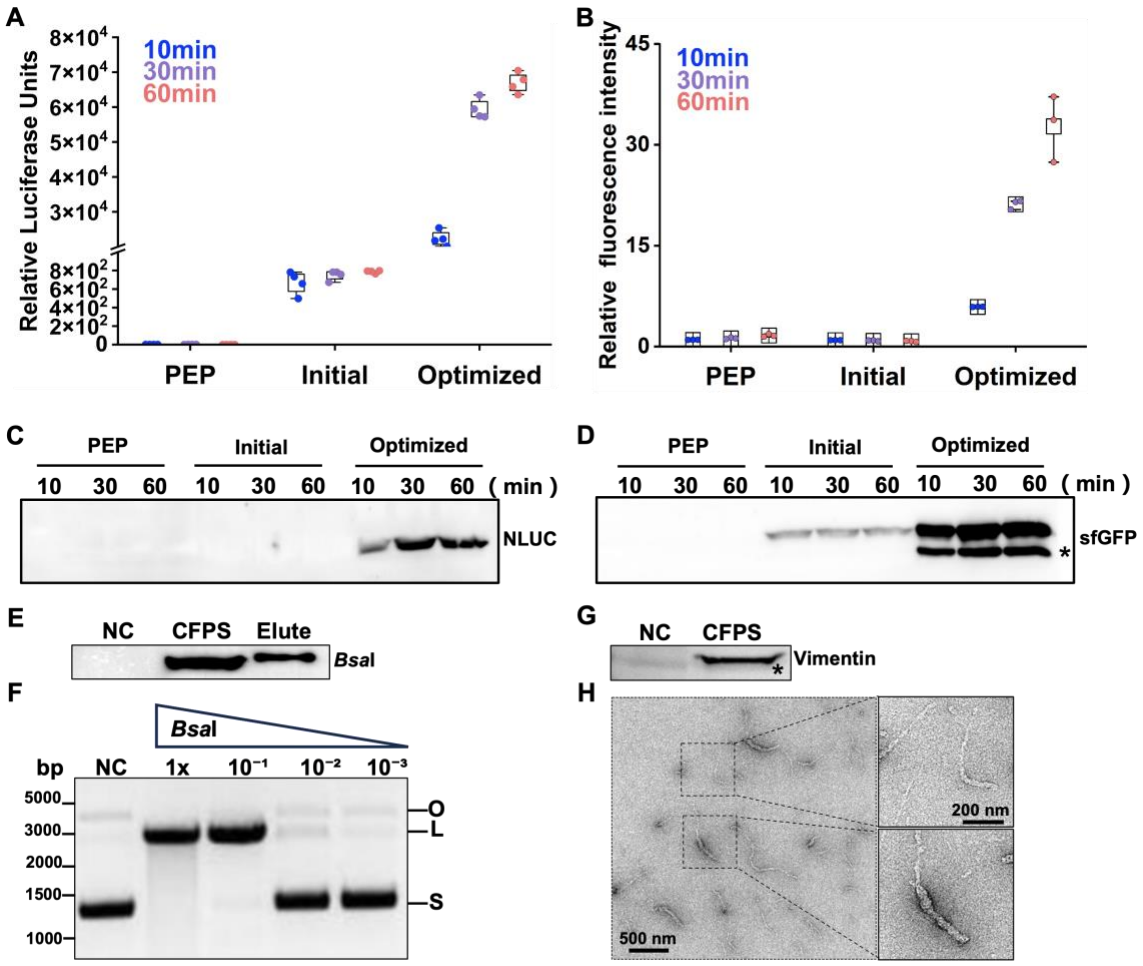

229

230 **Figure 4 Benchmarking the optimized *e*CFPS system with different DNA templates.**

231 **(A)** NLuc protein expression kinetics over time, comparing the PEP-based, initial
232 CrP/CrK-based, and optimized CrP/CrK-based energy regeneration systems. Data
233 present mean ± SE, n = 4. (**B**) sfGFP protein expression kinetics over time from the three
234 energy regeneration systems. Data present mean ± SE, n = 3. (**C-D**) Western blot
235 validation of protein expression for NLuc (**C**) and sfGFP (**D**) from the different *e*CFPS
236 system shown in (**A-B**). Protein products were detected using an anti-FLAG antibody.
237 The asterisk (*) indicates a non-specific band. (**E**) Western blot detection of His-FLAG-
238 *Bsa*I expressed by the optimized *e*CFPS system using an anti-FLAG antibody. (**F**)
239 Agarose gel electrophoresis confirming the functional activity of *e*CFPS-synthesized *Bsa*I
240 via cleavage of a substrate plasmid. A 10-fold serial dilution of *Bsa*I was with 1x
241 representing 0.05 mg/mL. NC (negative control) indicates no plasmid in the *e*CFPS
242 reaction. S, L, and O indicate the respective position of the supercoiled, linear, and open
243 circular forms of the plasmid. (**G**) Western blot analysis of vimentin expressed by the
244 optimized *e*CFPS system using an anti-vimentin antibody. (**H**) Negative-stain electron
245 microscopy image showing that vimentin expressed via *e*CFPS can successfully self-
246 assemble into filaments *in vitro*.

247 **A simplified method for bacterial lysate preparation and quality control**

248 In addition to optimizing the reaction buffer, we sought to simplify the entire *e*CFPS
249 procedure by developing an easy-to-use method for preparing the bacterial cell lysate.
250 During lysate making, traditional methods, which often rely on time-consuming runoff and
251 dialysis procedures[21,8], were replaced with a high-pressure homogenizer for efficient cell
252 disruption, eliminating the need for additional dialysis. Compared to traditional
253 biochemical methods such as ultrasonication, lysozyme treatment, or freeze-thaw
254 cycles[52], this approach is faster and more convenient (**Figure 5A**). Additionally,
255 endogenous T7 RNA polymerase in the optimized *e*CFPS lysate obviates exogenous
256 addition, simplifying preparation and reducing costs while maintaining high translation
257 efficiency (**Figure 5A**). We validated this new "fast lysate" preparation by rigorous quality
258 control. We tested lysates prepared from cells harvested at various optical densities at
259 600 nm (OD_{600}). While the density did not significantly impact protein expression levels,
260 a harvest optical density of OD_{600}=2 yielded the best performance (**Figure 5B**). The
261 quality of the lysate, particularly the integrity of its translational machinery, was further

262 confirmed by sucrose gradient centrifugation (**Figure S4A**) and negative-staining
263 transmission electron microscopy (TEM) images (**Figure S4B**) showing well-resolved
264 70S ribosomes.

265 To further simplify the protocol, we evaluated the necessity of the traditional runoff and
266 dialysis steps[8] (**Figure 5A**). Our results from sucrose gradient analysis and TEM imaging
267 confirmed that ribosomes remained intact, and the *e*CFPS expression signal was
268 significantly higher without them (**Figure 5C-D, Figure S4B**). These findings confirm that
269 both the runoff and dialysis steps are dispensable for our system, allowing for a
270 significantly simplified and faster preparation. Additionally, our reliance on endogenously
271 expressed T7 RNA polymerase yields a significantly higher expression signal,
272 outperforming previously reported *e*CFPS systems by up to four-fold (**Figure 5D**).

273 Our optimized lysate preparation method yielded highly active and stable extracts. It is
274 capable of sustaining protein synthesis for up to 120 minutes (**Figure S4C**) and maintains
275 protein synthesis efficiency even after multiple freeze-thaw cycles, making it highly
276 suitable for routine laboratory use (**Figure 5E**).

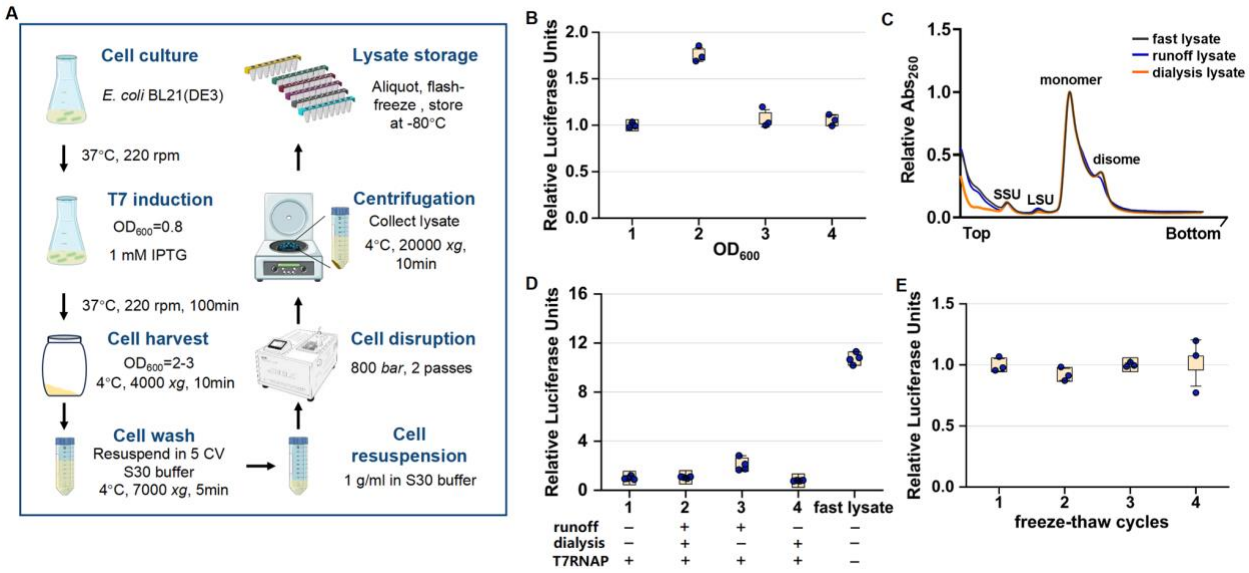

277

278 **Figure 5 Preparation of *e*CFPS from cultured *E. coli* Cells.** (**A**) Flowchart of the *e*CFPS
279 preparation procedures. (**B**) Comparison of reaction efficiency in *e*CFPS using lysate with
280 bacteria cells harvested at different optical density. Data present mean ± SE, n = 3. (**C**)
281 Sucrose gradient sedimentation analysis of different lysates used for *e*CFPS, revealing

282 the presence of ribosome monomers. (**D**) Comparison of protein expression levels in
283 *e*CFPS system using lysates prepared by runoff, dialysis, and rapid endogenous T7 RNA
284 polymerase induction. Data present mean ± SE, n = 4. (**E**) Comparison of reaction
285 efficiency in *e*CFPS using lysates after different numbers of freeze-thaw cycles. Data
286 present mean ± SE, n = 3.
287
288 **Discussion**

289 In this study, we successfully developed a highly streamlined and efficient *e*CFPS system.
290 By systematically eliminating dispensable components from traditional protocols, we
291 reduced the complexity of the reaction mixture from thirty-five to a core set of just seven
292 components. This simplification represents a significant advancement over conventional
293 systems by not only drastically lowering the cost and effort of preparing the reaction buffer,
294 but also by minimizing potential inhibitory interactions between numerous auxiliary
295 components, thereby making the system more accessible for a wider range of
296 researchers and laboratories.

297 The thorough optimization of the seven core components was a critical step in achieving
298 high protein expression levels. Our detailed screening of key factors like salts, energy
299 components, and buffer conditions revealed that precise concentrations are essential for
300 optimal performance. The synergistic effect of these optimized components was evident,
301 particularly the energy source and regeneration system, which is based on CrK coupled
302 with CrP[37]. A notable finding from our optimization was the ability of our system to function
303 effectively without certain components traditionally considered essential. For example,
304 the removal of DTT did not negatively impact protein expression, suggesting that our
305 lysate preparation procedure may maintain sufficient reducing conditions or that the high
306 expression levels are sufficiently rapid that protein aggregation is not a major issue.
307 Similarly, the ability to achieve high protein yields with minimal or even no added tRNA
308 or CTP/UTP highlights the remarkable robustness and inherent capacity of our lysate,
309 likely due to residual components retained during our simplified preparation method. We
310 also observed that the protein synthesis signal was significantly higher without traditional
311 runoff and dialysis steps, strongly suggesting that these steps may inadvertently remove
312 endogenous components essential for efficient protein synthesis. The high activity of this

313 "fast lysate," which retains essential endogenous components, is the key factor enabling
314 the dramatic simplification of the reaction buffer. This led to a significant improvement in
315 protein synthesis yield compared to both classical and initial systems.

316 The benchmarking experiments clearly demonstrated that our optimized *e*CFPS system
317 provides higher protein expression levels compared to these traditional systems while
318 offering faster kinetics, which is a key advantage for high-throughput applications. The
319 successful production of active *Bsa*I restriction enzyme, a cytosolic toxic and difficult-to-
320 express protein, and the functional assembly of vimentin, a difficult-to-handle intermediate
321 filament protein[51], further validate the superior robustness and translational quality of our
322 optimized system beyond simple reporters like Nluc.

323 Our simplified lysate preparation method, the novel “fast lysate” protocol which eliminates
324 the time-consuming runoff and dialysis steps, further distinguishes this work. We
325 demonstrate that a highly active lysate can be prepared rapidly using a high-pressure
326 homogenizer, which enhances the overall accessibility and robustness of our *e*CFPS
327 system. The ability to use the lysate directly after a single centrifugation step, coupled
328 with the reliance on endogenous T7 RNA polymerase, makes our protocol one of the
329 most straightforward and rapid for producing high-quality *e*CFPS lysates. This
330 streamlined preparation procedure is a significant step toward making CFPS a more
331 routine and scalable tool for diverse applications.

332 In conclusion, our optimized and streamlined *e*CFPS system represents a significant
333 advancement in the field of prokaryotic cell-free protein synthesis. By drastically reducing
334 the number of reaction components and simplifying the lysate preparation procedure, we
335 have created a highly efficient, cost-effective, and user-friendly platform. This system is
336 poised to accelerate fundamental research and facilitate high-throughput protein
337 engineering, compound screening, and diagnostic development. Future work will focus
338 on further characterizing the endogenous factors in the lysate that enable the high
339 efficiency of our system and exploring its use in novel synthetic biology applications.

340

341 **Methods**

342 **Plasmid construction**

343 All plasmids and primers used in this study are detailed in **Table S2**. The NLuc and sfGFP
344 reporter genes, each fused with a FLAG-tag, were cloned into a T7-driven expression
345 vector. The sfGFP gene was optimized for *E. coli* codon usage to ensure efficient
346 translation. The vector backbone was constructed using standard molecular biology
347 techniques.

348 The *Bsa*I linear DNA templates was constructed from three DNA fragments amplified by
349 PCR. To enhance template stability and mitigate nuclease degradation within the CFPS
350 system, approximately 300 bp sequences were incorporated upstream and downstream
351 of the *Bsa*I coding sequence. The fragments encoding the T7 promoter/upstream
352 sequence (Fragment 1) and the T7 terminator/downstream sequence (Fragment 2) were
353 amplified from the pJL1 plasmid. Separately, the gene fragment for the restriction
354 endonuclease *Bsa*I was amplified from the pUC_*Bsa*I plasmid (Fragment 3). These three
355 fragments were subsequently fused using overlap PCR to generate the final linear
356 template, which was confirmed to lack the recognition sequence for the target *Bsa*I
357 enzyme.

358 ***E. coli* cell culture and lysate preparation**

359 *E. coli* S30 cell lysate for CFPS was prepared using a simplified protocol adapted from a
360 previously reported method[8]. Briefly, *E. coli* BL21(DE3) was cultured in LB medium at
361 37°C with shaking. Once the OD_{600} reached 0.8, endogenous T7 RNA polymerase
362 expression was induced with 1 mM IPTG. The culture was then grown for an additional 2
363 hours before being harvested (when the OD_{600} reached 2-3). The cells were collected by
364 centrifugation at 4000 *g* for 10 minutes at 4°C. The cell pellet was washed with 5 volumes
365 of cold S30 buffer (10 mM HEPES-KOH pH 7.5, 14 mM $Mg(OAc)_2$, 60 mM KOAc) and
366 then resuspended in S30 buffer at a ratio of 1 mL per gram of wet cell paste. Cell lysis
367 was performed using a high-pressure homogenizer at 800 *bar* for two passes. The lysate
368 was then clarified by centrifugation at 20,000 *g* for 10 minutes at 4°C, and the resulting
369 supernatant, designated as the “fast lysate”, was collected without subsequent runoff or
370 dialysis steps. This omission ensures maximal retention of endogenous components,

371 contributing directly to the observed system efficiency. Lysate quality control was
372 assessed by (i) sucrose density gradient analysis and negative-staining TEM to confirm
373 the integrity of 70S ribosomes, and (ii) functional testing by monitoring the synthesis and
374 activity of the challenging restriction enzyme, *Bsa*I and vimentin. Finally, the fast lysate
375 was aliquoted and flash-frozen in liquid nitrogen before being stored at -80°C until use.

376 A step-by-step protocol is provided in the supplementary protocol.

377 **e*CFPS reactions for luciferase reporter assay**

378 The optimized *e*CFPS reaction was performed in a 10 μL total volume containing the
379 components listed in **Table S3** and **Table S4**. Plasmid of NLuc reporter gene was used
380 as the template.

381 **CFPS expression, protein purification and analysis**

382 Protein expression levels were quantified using NLuc and sfGFP reporter systems. NLuc
383 activity was measured with the Nano-Glo luciferase assay system (Promega). Reaction
384 mixtures were diluted as specified in the source data to prevent signal saturation and then
385 analyzed on a microplate luminometer (BERTHOLD, Centro XS3 LB 960) to obtain the
386 luminescence units as described previously[53,54]. SfGFP fluorescence was used to
387 quantify protein synthesis following the methods reported[55]. Briefly, 5 μL of the reaction
388 mixture was added to 195 μL of fluorescence assay buffer (20mM HEPES-KOH pH7.5,
389 100mM NaCl, 5mM magnesium glutamate). Fluorescence was measured on a Cell
390 Imaging Multimode Reader (BioTek, Cytation 5) with an excitation wavelength of 485 nm
391 and an emission wavelength of 528 nm.

392 Western blotting analysis was performed to confirm protein synthesis of the *e*CFPS
393 reactions. Synthesized proteins were detected using a primary anti-FLAG (Sigma, Cat#:
394 M185-3L). Chemiluminescence was detected using a Gel Imaging System (Tanon).

395 **Expression and purification of vimentin and *Bsa*I**

396 The gene for human vimentin (GenBank NP_003371.2) was sub-cloned into the
397 pET507a vector for expression. *Bsa*I (4 mL reaction) and vimentin (1 mL reaction)
398 proteins were synthesized using a CFPS system. The core reaction mixture for both

399 proteins consisted of 16 mM magnesium glutamate, 250 mM potassium glutamate, 1.2
400 mM ATP, 2.4 mM GTP, 80 mM CrP, 125 μg/ml CrK, 13.3 ng/μl or 7.2 ng/μl DNA
401 template, and 50% cell extract.

402 For *Bsa*I purification, the 4 mL reaction mixture was centrifuged at 20,000 *g*, and the
403 supernatant was incubated with 600 μl of Ni beads for 1 h at 4°C. The beads were washed
404 five times with 2 mL of wash buffer (40 mM HEPES-KOH pH 7.5, 50 mM imidazole, 500
405 mM NaCl). Elution was performed with 2 mL of elution buffer (40 mM HEPES-KOH pH
406 7.5, 500 mM imidazole, 500 mM NaCl). The eluted *Bsa*I was desalted using a column
407 (desalting buffer: 40 mM HEPES-KOH pH 7.5, 500 mM NaCl, 1 mM DTT), concentrated
408 to 1 mg/ml, and stored at -80°C in the presence of 10% glycerol. *Bsa*I enzymatic activity
409 was validated in a 20 μL reaction containing 2 μL of 10x rCutsmart (NEB), 2 μg of a
410 substrate plasmid, and *Bsa*I enzyme diluted in a 10-fold gradient. The reaction was
411 incubated at 37°C for 1 h and visualized via agarose gel electrophoresis.

412 Vimentin synthesis was carried out in a 5 mL nuclease-free tube with static incubation at
413 37°C for 13 h. The *Bsa*I synthesis was performed in a 10 mL nuclease-free tube at 30°C
414 with shaking at 150 rpm for 13 h.

415 **Vimentin filament assembly**

416 Vimentin, expressed via CFPS, was refolded and prepared for assembly through a multi-
417 step gradient dialysis protocol. The protein was dialyzed at room temperature in a buffer
418 (5 mM Tris−HCl pH 8.5, 1 mM EDTA, 0.1 mM EGTA, 5 mM β-ME) sequentially containing
419 6 M, 4 M, and 2 M urea, with each step lasting 30 min. Subsequent overnight dialysis was
420 performed at 4°C in the same buffer lacking urea. The protein was finally dialyzed for 1 h
421 at room temperature into 5 mM Tris pH 8.5, 5 mM β-ME, ensuring the protein was in its
422 tetramer configuration, after which the sample was concentrated. To initiate filament
423 assembly, 20 μl of the concentrated protein solution was quickly mixed with 20 μl of
424 assembly buffer (5 mM Tris pH 8.5, 170 mM NaCl, 100 mM KCl, 5 mM $MgCl_2$) in a 200
425 μl PCR tube. The assembly reaction was incubated for 1 h in a PCR thermocycler
426 preheated to 25°C before being immediately transferred to ice. Filament formation was
427 subsequently verified by negative-stain transmission electron microscopy.

428 **Negative-staining transmission electron microscopy (TEM)**

429 Samples from vimentin assembly, the TEM samples were prepared by negative staining.
430 A glow-discharged, carbon-coated copper grid was first rinsed with 3 μL of protein buffer
431 (5 mM Tris pH 8.5, 5 mM β−ME). Then, 3 μL of the assembled sample solution was
432 incubated on the grid for 20s. The sample was fixed using 3 μL of 0.8% glutaraldehyde
433 solution for 20s. Finally, the grid was stained twice with 3 μl of uranyl acetate solution,
434 with each staining step lasting 90 s. Samples were observed using a Talos F200C
435 transmission electron microscope at a nominal magnification of 92,000.

436 Samples from the SDG were prepared for TEM. Fresh, glow-discharged carbon-coated
437 grids were immersed in 3 μL of the corresponding sample for 2 minutes. Excess solvent
438 was removed, and the grids were stained with uranyl acetate for 1 minute and air dried.

439 **Sucrose density gradient (SDG) analysis**

440 A volume of 170–180 μL of lysate was loaded onto a 10%–40% (w/w) SDG. The gradient
441 buffer contained 10 mM HEPES-KOH (pH 7.5), 14 mM $Mg(OAc)_2$, 60 mM KOAc. The
442 gradient was prepared using a simple diffusion method (Biocomp) and centrifugation at
443 38,000 rpm for 2.5 hours at 4°C in a Beckman SW41Ti rotor. Following centrifugation, the
444 gradient was fractionated using a density gradient fractionation system (Biocomp), with
445 continuous monitoring of the absorbance at 260 nm.

446

447 **Acknowledgements**

448 We thank Alexey Amunts for helpful discussions. We also thank Jian Li and Wanqiu Liu
449 from Shanghai Tech University for providing the endonuclease plasmids and sharing the
450 linear fragment construction method. This work was supported by grants from the
451 National Key Research and Development Program of China (2022YFA0807100),
452 National Natural Science Foundation of China (32171291 and 32371351), Nature
453 Science Foundation of Shandong Province (ZR2021QC002) the Shandong Excellent
454 Young Scientists Fund Program (2022HWYQ-025), Taishan Scholars Program
455 (tsqnz20221104), Cutting Edge Development Fund of Advanced Medical Research
456 Institute (GYY2023QY01) and the Cheeloo Youth Program of Shandong University to
457 W.L..

Contributions

X.L.,C.Z. and J.L. were responsible for obtaining experimental data and performing data processing. X.L. and C.Z. conducted biochemical experiments. X.L., C.Z., Z.Z. and W.L. analyzed the data and created charts. W.L. wrote the initial draft of the paper. All authors edited the paper.

References

1. Carlson, E. D., Gan, R., Hodgman, C. E. & Jewett, M. C. Cell-free protein synthesis: applications come of age. *Biotechnol. Adv.* **30**, 1185–1194 (2012).
2. Katzen, F., Chang, G. & Kudlicki, W. The past, present and future of cell-free protein synthesis. *Trends Biotechnol.* **23**, 150–156 (2005).
3. Martin, R. W. *et al.* Cell-free protein synthesis from genomically recoded bacteria enables multisite incorporation of noncanonical amino acids. *Nat. Commun.* **9**, 1203 (2018).
4. Liu, C. C. & Schultz, P. G. Adding new chemistries to the genetic code. *Annu. Rev. Biochem.* **79**, 413–444 (2010).
5. Dumas, A., Lercher, L., Spicer, C. D. & Davis, B. G. Designing logical codon reassignment - Expanding the chemistry in biology. *Chem. Sci.* **6**, 50–69 (2015).
6. Guzman-Chavez, F. *et al.* Constructing cell-free expression systems for low-cost access. *ACS Synth. Biol.* **11**, 1114–1128 (2022).
7. Gregorio, N. E., Levine, M. Z. & Oza, J. P. A user's guide to cell-free protein synthesis. *Methods Protoc.* **2**, 24 (2019).
8. Jiang, N., Ding, X. & Lu, Y. Development of a robust Escherichia coli-based cell-free protein synthesis application platform. *Biochem. Eng. J.* **165**, 107830 (2021).
9. Xu, H., Liu, W.-Q. & Li, J. Translation related factors improve the productivity of a Streptomyces-based cell-free protein synthesis system. *ACS Synth. Biol.* **9**, 1221–1224 (2020).
10. Zemella, A., Thoring, L., Hoffmeister, C. & Kubick, S. Cell-free protein synthesis: Pros and cons of prokaryotic and eukaryotic systems. *Chembiochem* **16**, 2420–2431 (2015).
11. Jiang, L., Zhao, J., Lian, J. & Xu, Z. Cell-free protein synthesis enabled rapid prototyping for metabolic engineering and synthetic biology. *Synth. Syst. Biotechnol.* **3**, 90–96 (2018).
12. Endoh, T. *et al.* Cell-free protein synthesis at high temperatures using the lysate of a hyperthermophile. *J. Biotechnol.* **126**, 186–195 (2006).
13. Ji, X., Liu, W.-Q., Cao, Z., Huang, S. & Li, J. Establishing a high-yield Bacillus subtilis-based cell-free protein synthesis system for in vitro prototyping and natural product biosynthesis. *ACS Synth. Biol.* **14**, 1288–1297 (2025).
14. Gao W., Bu N. & Lu Y. Recent advances in cell-free unnatural protein synthesis. *Sheng Wu Gong Cheng Xue Bao* **34**, 1371–1385 (2018).
15. Lee, K.-H. & Kim, D.-M. Recent advances in development of cell-free protein synthesis systems for fast and efficient production of recombinant proteins. *FEMS Microbiol. Lett.* **365**, (2018).

16. Meng, Y., Yang, M., Liu, W. & Li, J. Cell-free expression of a therapeutic protein serratiopeptidase. *Molecules* **28**, 3132 (2023).
17. Kigawa, T. *et al.* Cell-free production and stable-isotope labeling of milligram quantities of proteins. *FEBS Lett.* **442**, 15–19 (1999).
18. Kim, J., Copeland, C. E., Seki, K., Vögeli, B. & Kwon, Y.-C. Tuning the cell-free protein synthesis system for biomanufacturing of monomeric human filaggrin. *Front. Bioeng. Biotechnol.* **8**, 590341 (2020).
19. Bothe, A. & Ban, N. A highly optimized human in vitro translation system. *Cell Rep. Methods* **4**, 100755 (2024).
20. Aleksashin, N. A., Chang, S. T.-L. & Cate, J. H. D. A highly efficient human cell-free translation system. *RNA* **29**, 1960–1972 (2023).
21. Levine, M. Z., Gregorio, N. E., Jewett, M. C., Watts, K. R. & Oza, J. P. Escherichia coli-Based Cell-Free Protein Synthesis: Protocols for a robust, flexible, and accessible platform technology. *J. Vis. Exp.* (2019) doi:10.3791/58882-v.
22. Sands, W. A. & Palmer, T. M. Regulating gene transcription in response to cyclic AMP elevation. *Cell. Signal.* **20**, 460–466 (2008).
23. Daniel, P. B., Walker, W. H. & Habener, J. F. Cyclic AMP signaling and gene regulation. *Annu. Rev. Nutr.* **18**, 353–383 (1998).
24. Boshart, M., Weih, F., Schmidt, A., Fournier, R. E. & Schütz, G. A cyclic AMP response element mediates repression of tyrosine aminotransferase gene transcription by the tissue-specific extinguisher locus Tse-1. *Cell* **61**, 905–916 (1990).
25. Chu, I.-T., Hutcheson, B. O., Malsch, H. R. & Pielak, G. J. Macromolecular crowding by polyethylene glycol reduces protein breathing. *J. Phys. Chem. Lett.* **14**, 2599–2605 (2023).
26. Ge, X., Luo, D. & Xu, J. Cell-free protein expression under macromolecular crowding conditions. *PLoS One* **6**, e28707 (2011).
27. Liebau, J. *et al.* Polyethylene glycol impacts conformation and dynamics of Escherichia coli prolyl-tRNA synthetase via crowding and confinement effects. *Biochemistry* **63**, 1621–1635 (2024).
28. Paudel, B. P., Fiorini, E., Börner, R., Sigel, R. K. O. & Rueda, D. S. Optimal molecular crowding accelerates group II intron folding and maximizes catalysis. *Proc. Natl. Acad. Sci. U. S. A.* **115**, 11917–11922 (2018).
29. Zhang, L., Lin, X., Wang, T., Guo, W. & Lu, Y. Development and comparison of cell-free protein synthesis systems derived from typical bacterial chassis. *Bioresour. Bioprocess.* **8**, 58 (2021).
30. Auton, M., Rösgen, J., Sinev, M., Holthauzen, L. M. F. & Bolen, D. W. Osmolyte effects on protein stability and solubility: a balancing act between backbone and side-chains. *Biophys. Chem.* **159**, 90–99 (2011).
31. Mojtabavi, S., Samadi, N. & Faramarzi, M. A. Osmolyte-induced folding and stability of proteins: Concepts and characterization. *Iran. J. Pharm. Res.* **18**, 13–30 (2019).
32. Hunt, A. C. *et al.* Cell-free gene expression: Methods and applications. *Chem. Rev.* **125**, 91–149 (2025).

33. Cai, Q. *et al.* A simplified and robust protocol for immunoglobulin expression in Escherichia coli cell-free protein synthesis systems. *Biotechnol. Prog.* **31**, 823–831 (2015).
34. Anderson, W. F. The effect of tRNA concentration on the rate of protein synthesis. *Proc. Natl. Acad. Sci. U. S. A.* **62**, 566–573 (1969).
35. Deutscher, M. P. Processing of tRNA in prokaryotes and eukaryotes. *CRC Crit. Rev. Biochem.* **17**, 45–71 (1984).
36. Rodnina, M. V. Translation in prokaryotes. *Cold Spring Harb. Perspect. Biol.* **10**, (2018).
37. Kim, D. M. & Swartz, J. R. Prolonging cell-free protein synthesis by selective reagent additions. *Biotechnol. Prog.* **16**, 385–390 (2000).
38. Kim, D. M. & Swartz, J. R. Prolonging cell-free protein synthesis with a novel ATP regeneration system. *Biotechnol. Bioeng.* **66**, 180–188 (1999).
39. Agirrezabala, X. & Frank, J. Elongation in translation as a dynamic interaction among the ribosome, tRNA, and elongation factors EF-G and EF-Tu. *Q. Rev. Biophys.* **42**, 159–200 (2009).
40. Mayer, M. P. The Hsp70-chaperone machines in bacteria. *Front. Mol. Biosci.* **8**, 694012 (2021).
41. Nierhaus, K. H. Mg2+, K+, and the ribosome. *Journal of bacteriology* vol. 196 3817–3819 (2014).
42. Gesteland, R. F. Unfolding of Escherichia coli ribosomes by removal of magnesium. *J. Mol. Biol.* **18**, 356–371 (1966).
43. Espinasse, A., Lembke, H. K., Cao, A. A. & Carlson, E. E. Modified nucleoside triphosphates in bacterial research for in vitro and live-cell applications. *RSC Chem. Biol.* **1**, 333–351 (2020).
44. Calhoun, K. A. & Swartz, J. R. An economical method for cell-free protein synthesis using glucose and nucleoside monophosphates. *Biotechnol. Prog.* **21**, 1146–1153 (2005).
45. Sitaraman, K. *et al.* A novel cell-free protein synthesis system. *J. Biotechnol.* **110**, 257–263 (2004).
46. Gaddi, A. V., Galuppo, P. & Yang, J. Creatine phosphate administration in cell energy impairment conditions: A summary of past and present research. *Heart Lung Circ.* **26**, 1026–1035 (2017).
47. Wallimann, T., Tokarska-Schlattner, M. & Schlattner, U. The creatine kinase system and pleiotropic effects of creatine. *Amino Acids* **40**, 1271–1296 (2011).
48. Hochuli, E., Bannwarth, W., Döbeli, H., Gentz, R. & Stüber, D. Genetic approach to facilitate purification of recombinant proteins with a novel metal chelate adsorbent. *Nat. Biotechnol.* **6**, 1321–1325 (1988).
49. Watanabe, N., Takasaki, Y., Sato, C., Ando, S. & Tanaka, I. Structures of restriction endonuclease HindIII in complex with its cognate DNA and divalent cations. *Acta Crystallogr. D Biol. Crystallogr.* **65**, 1326–1333 (2009).
50. Danna, K. & Nathans, D. Specific cleavage of simian virus 40 DNA by restriction endonuclease of Hemophilus influenzae. *Proc. Natl. Acad. Sci. U. S. A.* **68**, 2913–2917 (1971).
51. Eibauer, M. *et al.* Vimentin filaments integrate low-complexity domains in a complex helical structure. *Nat. Struct. Mol. Biol.* **31**, 939–949 (2024).

591 52. Fujiwara, K. & Doi, N. Biochemical preparation of cell extract for cell-free protein
592 synthesis without physical disruption. *PLoS One* **11**, e0154614 (2016).
593 53. Li, W. *et al.* Structural basis for selective stalling of human ribosome nascent chain
594 complexes by a drug-like molecule. *Nat. Struct. Mol. Biol.* **26**, 501–509 (2019).
595 54. Wu, M. *et al.* Human ribosome interactions reframe neomycin toxicity. *bioRxiv*
596 (2025) doi:10.1101/2025.07.22.666027.
597 55. Wang, Y., Wang, T., Chen, X. & Lu, Y. IRES-mediated Pichia pastoris cell-free
598 protein synthesis. *Bioresour. Bioprocess.* **10**, 35 (2023).